THE SIMULATION OF ONE-DIMENSIONAL SHALLOW WATER WAVE EQUATION WITH MACCORMACK SCHEMES

Iffah Nurlathifah Fikri[1*], Sumardi[2]

[1,2] *Mathematics Study Program, Faculty of Mathematics and Natural Sciences, Universitas Gadjah Mada*
Sekip Utara Bulaksumur Kotak Pos 21, Geografi St., Senolowo, Sinduadi, Mlati, Sleman, Yogyakarta, 55281, Indonesia

Corresponding author's e-mail: [1]* iffah.n.f@mail.ugm.ac.id

Abstract. *Many practical problems can be modeled using the one-dimensional shallow water wave equation. Therefore, the solution to the one-dimensional shallow water wave equation will be discussed to solve this problem. The research method used was the study of literature related to the shallow water wave equation and its solution method. The one-dimensional shallow water wave equation can be derived from the law of conservation of mass and the law of conservation of momentum. In this study, one of the finite difference methods will be discussed, namely the MacCormack method. The MacCormack method consists of two steps, namely the predictor and corrector steps. The MacCormack method was used to perform numerical simulations of the pond and tsunami models for one-dimensional (1D) shallow water wave equations with flat and non-flat topography. The simulation results showed that the channel's topography could affect the water surface's height and velocity. At the same time, a channel with a non-flat topography had a slower water velocity than the water velocity of a channel with a flat topography.*

Keywords: MacCormack method, pond, shallow water wave, topography, tsunami.

1. INTRODUCTION

A mathematical model can express many phenomena around us. A mathematical model is a way to express a phenomenon in the form of a mathematical formula so that it is easy to learn and perform calculations. One of the models of water waves was studied in this study, namely shallow-water waves. Shallow water waves are water waves that have a water depth of less than 1/20 of the wavelength, whose speed is affected by the depth of the water [1]. The practical problems of shallow water waves include the spread of tsunami waves, ripples in pond water, and the collapse of dams. Judging from the many problems that can be applied to shallow water waves, it is necessary to discuss the search for a solution to the shallow water wave equation [2].

This study's shallow water wave equation applies to fluids with a constant density, are not vicious, flow without rotation, and cannot be compressed [3]. The laws of physics related to the shallow water wave equation are the laws of conservation of mass and momentum. The shallow water wave equation consists of two equations. The first equation is the continuity equation derived from the law of conservation of mass, and the second is the momentum equation derived from the law of conservation of momentum. The shallow water equation takes the form of a first-order nonlinear system of partial differential equations [4].

Many researchers have studied the solution to the shallow water wave equation using numerical methods. Numerical simulation of the 1D and 2D cases of shallow water wave equations of tsunami models using the finite volume method of the Godunov type has been discussed by [2]. Furthermore, research on solving 1D and 2D shallow water wave equations with several models, such as a collapsed dam on a dry sloping bottom using the staggered grid volume method, has been discussed by [5], [6]. Then, the 1D shallow water wave equation simulation using the Lax-Friedrichs method was studied by [3] and [7]. Furthermore, the solution of the 1D shallow water wave equation using the WENO finite difference method has been studied by [4]. In contrast, [8] uses the ordinary finite difference method. In addition, in this research article, we discussed the 1D shallow water wave equation simulation using a different numerical method from the studies above.

The numerical method that was used to solve the 1D shallow water wave equation is the MacCormack finite difference method. Robert W. MacCormack introduced this method in 1969 through his publication entitled "The Effect of Viscosity in Hypervelocity Impact Cratering." MacCormack method can be used to solve the fluid flow model [9], pollution model [10], and water flow model (shallow water wave equation) [11]. In addition, the MacCormack method has second-order accuracy [9] and good simulation results [11], [12].

The problems of shallow water waves that will be discussed are the spread of tsunami waves and disturbed pond water [13]. Tsunamis are generated by the displacement of large volumes of water due to earthquakes, volcanic eruptions, landslides, or other causes above or below the seabed. In general, the characteristics of a tsunami wave have a wavelength much larger than the structure of the depth of the sea that it passes through [2], [14], [15]. Therefore, the topography of the seabed will be higher if it is closer to the coast. Therefore, it will cause a large difference in the amplitude of the tsunami wave when it is close to the coast compared to far from the coast or in the high seas [1]. Furthermore, the case that the surface of the pond water, which initially tends to be calm, will cause shallow-water waves when disturbed [3]. In the case of pond water, the difference in the distribution of water waves for flat and non-flat topography will also be studied [6]. Then, analysis and interpretation of the simulation results for the two problems above will be carried out, namely the distribution of tsunami waves and disturbed pond water. The simulation results are wave speed data, wave distance, and water depth at a certain time interval.

The simulation results revealed the speed and distance of the waves in the two models, pond and tsunami, for two cases, namely flat and non-flat topography, as well as the difference between flat and non-flat topography in each model. This research can support further studies by expanding the shallow water wave equation model to be multi-dimensional using the MacCormack method with flat and non-flat topography.

2. RESEARCH METHOD

The method used in this article was a literature study. It was started by searching and studying the literature in the form of books, articles, and journals related to the one-dimensional shallow water wave equation and the MacCormack method. Then, the MacCormack method was used to simulate a shallow water wave equation problem. After studying the available literature, the steps taken were as follows:

2.1. Deriving the 1D Shallow Water Wave Equation

The shallow water wave equation consists of the continuity equation and the momentum equation, which can be derived from the law of conservation of mass and the law of conservation of momentum, respectively. Based on Figure 1, we used space variable x and time variable t. The topography of the soil is $z(x)$, the depth of water at point x and at time t is $h(x,t)$, The height of the free water wave surface is $H(x,t) = z(x) + h(x,t)$ and the velocity of the water flow at point x at time t is $u(x,t)$.
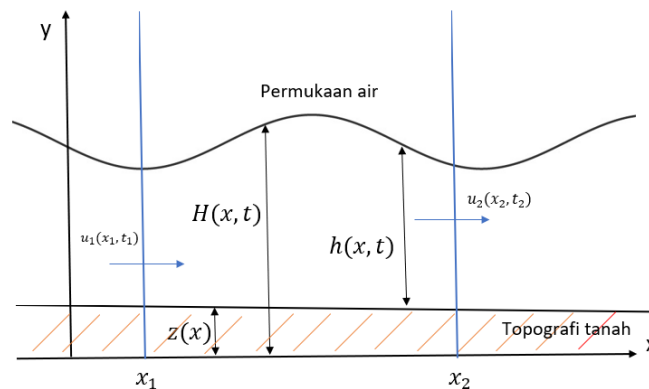

Figure 1. One-dimensional (1D) shallow water wave illustration

Assuming that the wave propagates on a free surface, the uniform density ρ, the frictional force is neglected, and does not depend on the y-dimensional space, then the following system of differential equations:

$$\frac{\partial h}{\partial t} + \frac{\partial (hu)}{\partial x} = 0$$
$$\frac{\partial (hu)}{\partial t} + \frac{\partial \left(hu^2 + \frac{1}{2}gh^2 \right)}{\partial x} = -gh\frac{\partial z}{\partial x}, \tag{1}$$

is called the one-dimensional (1D) shallow water wave equation with the acceleration due to gravity g, dependent variables u, h and z as well as independent variables x and t.

Based on [5], it is given a system of equations which is equivalent to the following Equations System (1):

$$\frac{\partial \eta}{\partial t} + \frac{\partial \big(u(D + \eta) \big)}{\partial x} = 0$$
$$\frac{\partial u}{\partial t} + u\frac{\partial u}{\partial x} = -g\frac{\partial \eta}{\partial x}. \tag{2}$$

The first equation in the system of Equations (2) is the continuity equation, while the second equation describes the motion, which is the evolution of the velocity u in the x direction. The model can be illustrated as in Figure 2. In the Equation System (2), η is the elevation of the water surface, which is positive if it is above the equilibrium level, D is a function of the water depth, which is positive if it is below the equilibrium level. Look at Figure 2, the equilibrium level is the water level line when it is calm. The total water depth is $D + \eta$.
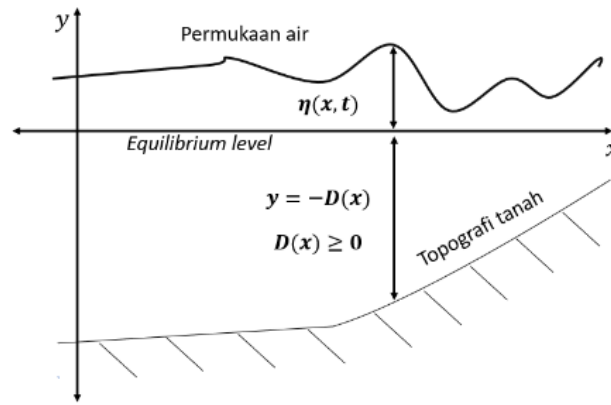
Figure 2. Illustration of the equations system modelling (2)

2.2. Deriving MacCormack's Method Approach for the 1D Shallow Water Wave

Before deriving the approximation formula for the MacCormack method for the shallow water wave equation, it was defined:

$$\Delta x = \frac{L}{N_x}, \qquad x_i = x_0 + i\Delta x; i = 0, 1, 2, \dots, N_x,$$
$$\Delta t = \frac{L}{N_t}, \qquad x_i = n\Delta t; n = 0, 1, 2, \dots, N_t,$$

with L flow length, T time duration, N_x number of discretization of space variables, and N_t number of time variable discretization. Thus, the discretization of the dependent variable $\eta(x,t)$ and $u(x,t)$ at the point (x_i, t_n) and $D(x)$ at the point x_i denoted successively as η_i^n, u_i^n and D_i.

First, the predictor equation of the MacCormack method would be derived from the System of Equations (2). The first-order forward finite difference scheme was used to approximate the partial derivatives of space and time variables in the System of Equations (2). The partial derivatives of space and time variables in the System of Equations (2) were approximated by a one-step forward difference scheme, so that the following equation was obtained.

$$\frac{\eta_i^{n+1} - \eta_i^n}{\Delta t} + \frac{u_{i+1}^n (D_{i+1} + \eta_{i+1}^n) - u_i^n (D_i + \eta_i^n)}{\Delta x} = 0,$$
$$\frac{u_i^{n+1} - u_i^n}{\Delta t} + u_i^n \frac{u_{i+1}^n - u_i^n}{\Delta x} = -g\left(\frac{\eta_{i+1}^n - \eta_i^n}{\Delta x}\right). \tag{3}$$

In the predictor step, the value of η_i^{n+1} and u_i^{n+1} is a temporary value at the time level $n+1$, so use the notation $\eta_i^{\overline{n+1}}$ and $u_i^{\overline{n+1}}$. Equation (3) can be written as:

$$\eta_i^{\overline{n+1}} = \eta_i^n - \alpha\big(u_{i+1}^n (D_{i+1} + \eta_{i+1}^n) - u_i^n (D_i + \eta_i^n)\big),$$
$$u_i^{\overline{n+1}} = u_i^n - \alpha u_i^n (u_{i+1}^n - u_i^n) - g\alpha(\eta_{i+1}^n - \eta_i^n), \tag{4}$$

With $\alpha = \frac{\Delta t}{\Delta x}$. Equation (4) is the predictor equation of the MacCormack method of the System of Equation (2).

Next, the corrector equation of the MacCormack method was derived from the System of Equations (2). The first-order backward finite difference scheme was used to approximate the partial derivatives of space and time variables. Then, the partial derivatives of space and time variables in the System of Equations (2) were approached successively with a one-step backward difference scheme and a half-step backward difference scheme so that we get:

$$\frac{\eta_i^{n+1} - \eta_i^{n+\frac{1}{2}}}{\frac{\Delta t}{2}} + \frac{u_i^{n+1} (D_i + \eta_i^{n+1}) - u_{i-1}^{n+1}(D_{i-1} + \eta_{i-1}^{n+1})}{\Delta x} = 0, \tag{5}$$

$$\frac{u_i^{n+1} - u_i^{n+\frac{1}{2}}}{\frac{\Delta t}{2}} + u_i^{n+1} \frac{u_i^{n+1} - u_{i-1}^{n+1}}{\Delta x} = -g\left(\frac{\eta_i^{n+1} - \eta_{i-1}^{n+1}}{\Delta x}\right).$$

Next, the value of $\overline{\eta_i^{n+1}}$ and $\overline{u_i^{n+1}}$ were used from the predictor step to replace the input value of Equation (5), so it can be written as:

$$\eta_i^{n+1} = \eta_i^{n+\frac{1}{2}} - \frac{\alpha}{2}\left(\overline{u_i^{n+1}}\left(D_i + \overline{\eta_i^{n+1}}\right) - \overline{u_{i-1}^{n+1}}\left(D_{i-1} + \overline{\eta_{i-1}^{n+1}}\right)\right),$$

$$u_i^{n+1} = u_i^{n+\frac{1}{2}} - \frac{\alpha \overline{u_i^{n+1}}}{2}\left(\overline{u_i^{n+1}} - \overline{u_{i-1}^{n+1}}\right) - \frac{g\alpha}{2}\left(\overline{\eta_i^{n+1}} - \overline{\eta_{i-1}^{n+1}}\right),$$

(6)

with $\alpha = \frac{\Delta t}{\Delta x}$. The value of $\eta_i^{n+\frac{1}{2}}$ and $u_i^{n+\frac{1}{2}}$ were replaced by the average value of η and u at the time level n with a temporary value at the time level $n + 1$, so that Equation (6) becomes:

$$\eta_i^{n+1} = \frac{1}{2}\left(\eta_i^n + \overline{\eta_i^{n+1}} - \alpha\left(\overline{u_i^{n+1}}\left(D_i + \overline{\eta_i^{n+1}}\right) - \overline{u_{i-1}^{n+1}}\left(D_{i-1} + \overline{\eta_{i-1}^{n+1}}\right)\right)\right),$$

$$u_i^{n+1} = \frac{1}{2}\left(u_i^n + \overline{u_i^{n+1}} - \alpha\overline{u_i^{n+1}}\left(\overline{u_i^{n+1}} - \overline{u_{i-1}^{n+1}}\right) - g\alpha\left(\overline{\eta_i^{n+1}} - \overline{\eta_{i-1}^{n+1}}\right)\right),$$

(7)

with $\alpha = \frac{\Delta t}{\Delta x}$. Equation (7) is the corrector equation of the MacCormack method of the System of Equations (2).

A stencil diagram of the one-dimensional (1D) MacCormack method is presented in Figure 3. In calculating the value of $\overline{\eta_i^{n+1}}$ and $\overline{u_i^{n+1}}$ in the predictor Equation (4) it takes two values of the water level elevation at the time level n (η_i^n, η_{i+1}^n), two values of wave velocity at the time level n (u_i^n, u_{i+1}^n) and two water depth values (D_i, D_{i+1}). Meanwhile, in finding the value of η_i^{n+1} and u_i^{n+1} in the corrector Equation (7) it takes the value of the water surface elevation and wave velocity at the time level n (η_i^n, u_i^n), temporary values of water surface elevation and wave velocity at time level $n + 1$ ($\overline{\eta_{i-1}^{n+1}}, \overline{\eta_i^{n+1}}, \overline{u_{i-1}^{n+1}}, \overline{u_i^{n+1}}$) and it takes two water depth values (D_{i-1}, D_i). Based on the initial conditions of the problem in the System of Equations (2), it can be obtained the value of η_i^0 and u_i^0 for $i \in \{0, 1, 2, .., N_x\}$. Meanwhile, the value of $\eta_0^n, u_0^n, \eta_{N_x}^n$ and $u_{N_x}^n$ can be obtained from the boundary conditions of the problem in the System of Equations (2) for $n \in \{0, 1, 2, ..., N_t\}$.
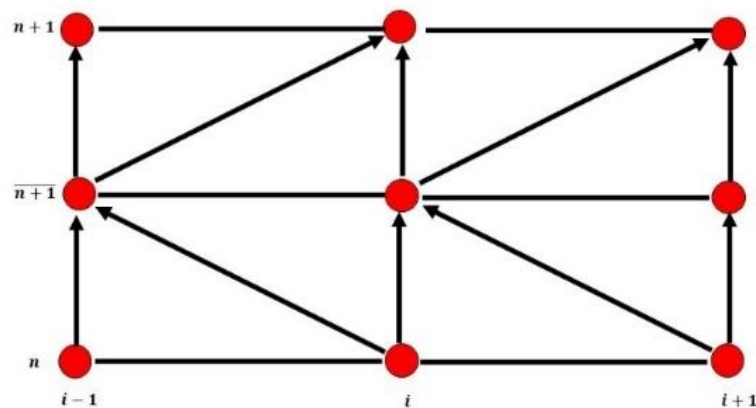

Figure 3. One-dimensional (1D) MacCormack stencil diagram for System of Equations (2)

2.3. Simulating the Shallow Water Wave Equation Using the MacCormack Method

One-dimensional shallow water wave equation simulation was carried out for two models, the pond model, and the Tsunami model, respectively, with flat and non-flat topography. This simulation uses the PYTHON programming language. Furthermore, analysis and interpretation of the simulation results were carried out.

3. RESULTS AND DISCUSSION

This section will discuss the numerical simulation results of the one-dimensional (1D) shallow water wave equation with flat and non-flat topography. Then, approach Equation (4) and Equation (7) were used to solve the problem with the help of PYTHON software. The problems to be discussed were the ripples in the pond water and the spread of the tsunami waves.

3.1. Pond Model

A simulation of the pond model for one-dimensional (1D) shallow water waves, where at first the water surface has zero or calm velocity. Then, it is disturbed in the form of initial waves. In this model, the water waves that hit the pond wall will always be reflected. As the result, the boundary conditions used were reflective boundary conditions. Suppose the pond has length L (in meters(m)), the computational domain for the variable space x was $\left[-\frac{L}{2}, \frac{L}{2}\right]$. The initial wave was in the middle of the pond. In other words, the crest of the initial wave was at $x = 0$. Space limit $x = -\frac{L}{2}$ and $x = \frac{L}{2}$ represents the pond wall. Meanwhile, the time used for the simulation is t (in seconds(s)) with the computational domain for the time variable t is $[0, T]$ with acceleration due to gravity $g = 9.8 \text{ m}/s^2$. In this model, the length of one unit of space x and time is equal to 10 meters and 1 s, respectively. As a result, the acceleration due to gravity g used is 0.98 unit space $/s^2$.

3.1.1. Flat Topography

The pond has a water depth below the *x*-axis (*equilibrium level)* follow function

$$D(x) = 0.08042, \; -2 \le x \le 2.$$

The Initial conditions for η and u was in the form of $\eta(x, 0) = 0.05e^{-x^2}$ and $u(x, 0) = 0$ for each $-2 \le x \le 2$. It will be observed the movement of water waves in the pond for 60 s using the reflective boundary conditions. Thus, the computational domain used in the experiment is $[-2,2] \times [0,60]$. The discretization of the initial and boundary conditions can be written as

$$\begin{matrix} \eta_i^0 = 0.05e^{-x_i^2} \\ u_i^0 = 0 \end{matrix} \qquad ; i = 0,1,2,\dots,N_x \qquad (8)$$

and

$$\begin{matrix} \eta_0^n = \eta_1^n, \eta_{N_x}^n = \eta_{N_x-1}^n \\ u_0^n = -u_1^n, u_{N_x}^n = -u_{N_x-1}^n \end{matrix} \qquad ; i = 0,1,2,\dots,N_t \qquad (9)$$

With $N_x = 200$ and $N_t = 3000$ so that the grid size was obtained $\Delta x = 0.02$ and $\Delta t = 0.02$.
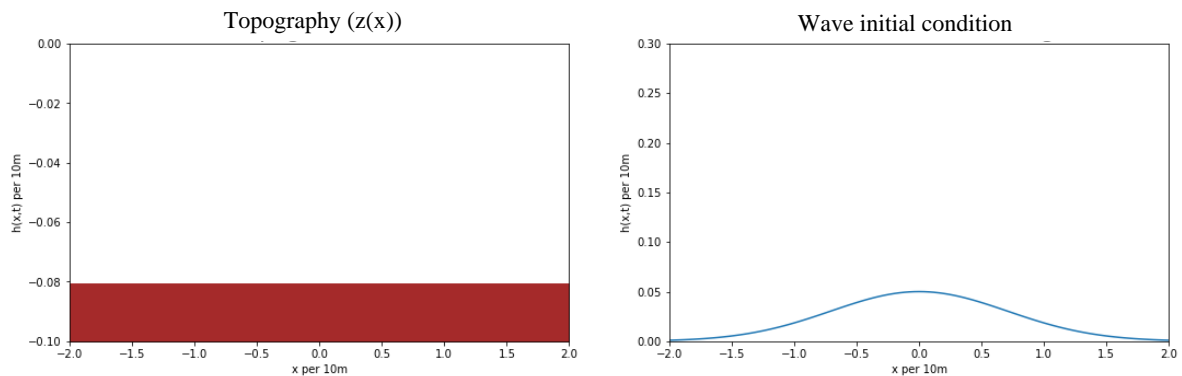

Figure 4. Bottom topography (left) and initial state of water level (right) for problem ponds with flat topography

Based on the initial conditions and the function of the water depth, the topography and initial conditions of the pond water surface are presented in Figure 4. It can be seen that the initial wave is a wave that has a large wavelength when compared to the depth of the pond water and is symmetrical to the center of the pond. Further numerical calculations were carried out using the MacCormack method with Equations (4) and (7).

The results of the numerical simulation of the pond model in this experiment at $t = 0,20,40,60$ are presented in Figure 5.
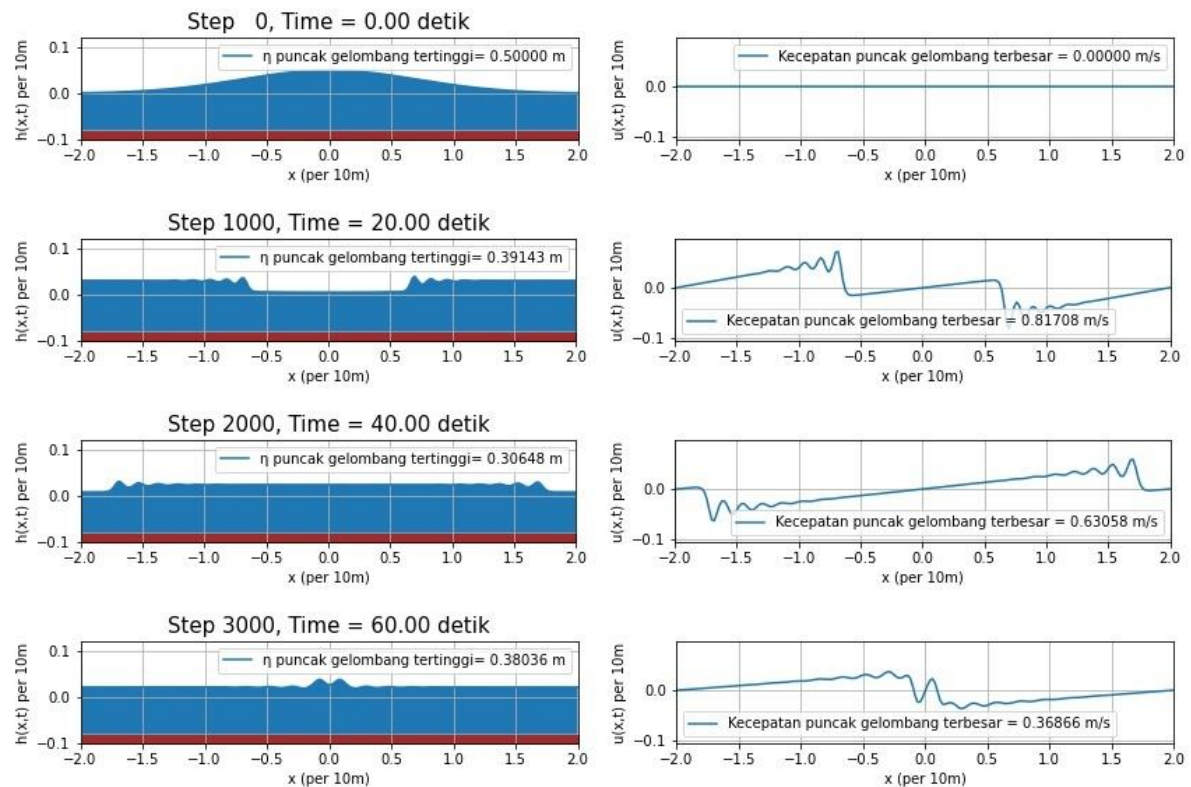

Figure 5. Depth (left) and velocity (right) of water in a pond for 60 s for flat topography

The simulation results show that the amplitude and speed of the waves on the surface of the water will always change. The reflective boundary conditions in this experiment cause the surface of the water that moves against the pond wall to move in the opposite direction towards the pond's center. At first, the surface of the pond water is calm with a speed of 0 m/s. Then, the pond surface began to move towards the pond wall when the water waves started to occur. Velocity will be positive when the water flows to the right and negative if vice versa. The average score η and the wave speed after reaching the last pond wall until $t = 60$ s in a row is 0.2223 m and 0.1279 m/s. Furthermore, the wave on the right of the pond will be called the right wave, analogous to the wave on the left of the pond is called the left wave

Furthermore, based on the simulation results, data on the distance of the left and right wave crests to the center of the pond are also obtained which are presented in Table 1 and η of the left and right waves have an average difference of 0.0111 m. Based on Table 1, the movement of water flow is symmetrical, with the distance of the left and right wave crests having the same value in x space units. In addition to peak distance data, the peak velocity of the left and right waves has a difference of 0.0259 m/s. Then, the difference in η and the peak velocity of the left and right waves is 0.0111 m and 0.0259 m/s, respectively. Finally, it is known that the average value of and the wave velocity after reaching the last pond wall until $t = 60$ s are 0.2223 m and 0.1279 m/s, respectively.

Table 1. Distance of left and right wave crests to the center of the pond with flat topography

t (s)	Distance to pond center (m)	
	Left wave crest distance	Right wave crest distance
6	2	2
15	1.7	1.7
24	0.58	0.58
33	0.54	0.54
42	1.66	1.66
51	1.18	1.18
60	0.08	0.08

3.1.2. Non-flat Topography

The pond has a water depth below the x axis (*equilibrium level*) follow function

$$D(x) = 0.002(x + 1.9)^2 + 0.05, \quad -2 \le x \le 2.$$

The initial condition for η and u are of in the form of $\eta(x, 0) = 0.05e^{-x^2}$ and $u(x, 0) = 0$ for each $-2 \le x \le 2$. The movement of water waves in the pond for 60 s was observed using the reflective boundary conditions. Thus, the computational domain used in the experiment is $[-2,2] \times [0,60]$. Discretization of the initial and boundary conditions, respectively, as in equation (8) and (9) with $N_x = 200$ and $N_t = 3000$, so that the grid size is obtained $\Delta x = 0.02$ and $\Delta t = 0.02$.
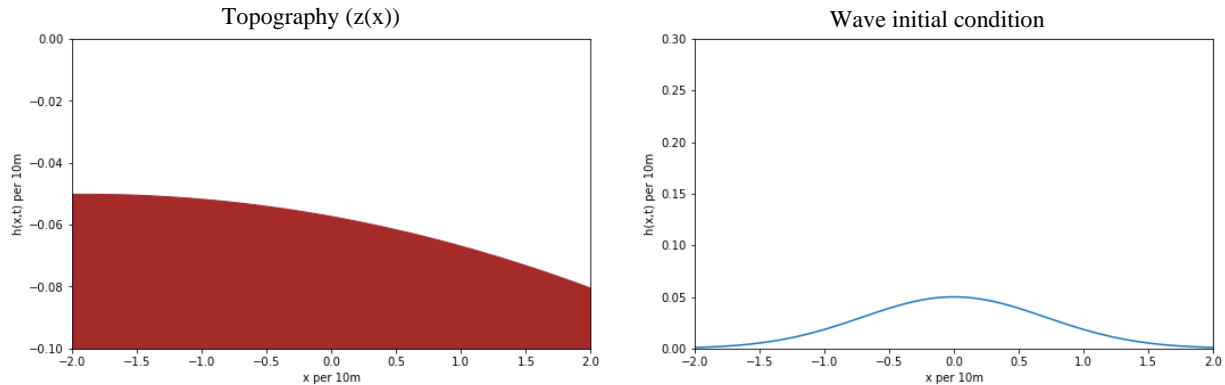

Figure 6. Topography of soil (left) and initial condition of pond water level (right) for problem ponds with uneven topography

Based on the initial conditions and the function of the water depth, the pond's bottom topography and the water surface's initial state are obtained, as shown in **Figure 6.** It can be seen that the initial wave is a wave that has a large wavelength when compared to the depth of the pond water and is symmetrical to the center of the pond. The topography of the pond is not as flat as in this case. Further numerical calculations were carried out using the MacCormack method with Equations (4) and (7). The results of the numerical simulation of the pond model in this experiment at $t = 0,20,40,60$ are presented in **Figure 7**.
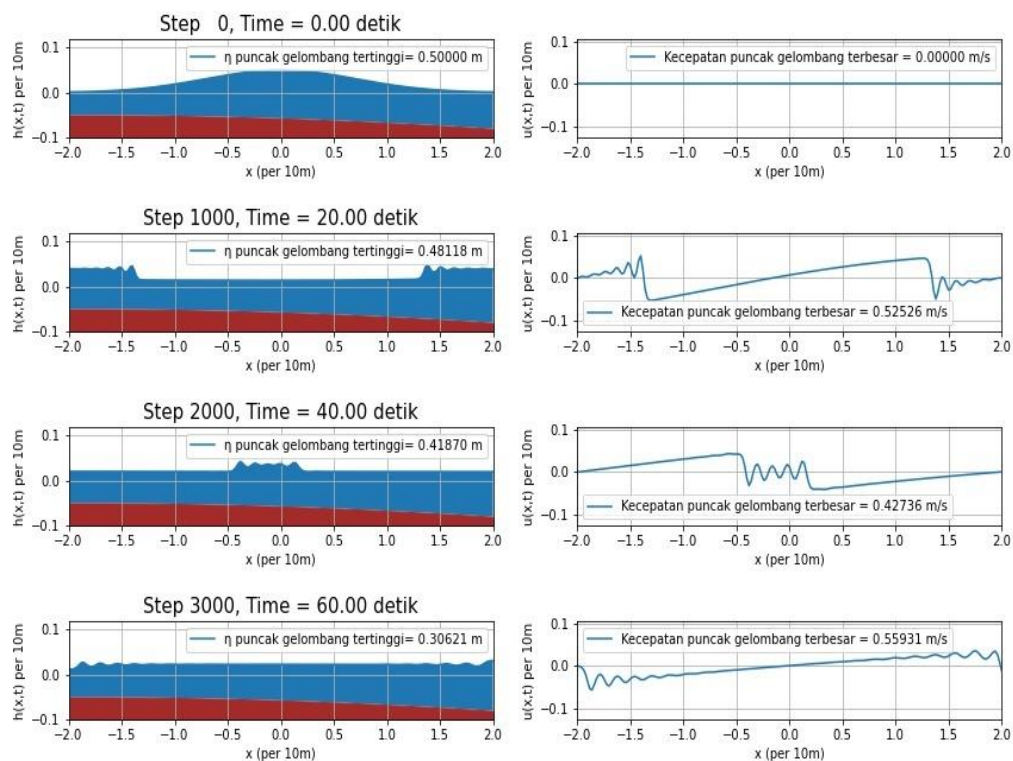

Figure 7. Depth (left) and velocity (right) of water in a pond for 60 s for non-flat topography

Based on the simulation results, the amplitude and speed of the waves on the surface of the water will always change. The reflective boundary conditions in this experiment cause the surface of the water that moves against the pond wall to move in the opposite direction towards the pond's center. At first, the surface of the pond water is calm with a speed of 0 m/s. Then, the pond surface begins to move towards the pond wall when the water waves start to occur. Velocity will be positive when the water flows to the right and negative otherwise. The average value and flow velocity before reaching the last pond wall until $t = 60$ s were 0.2214 m and 0.1250 m/s, respectively. Furthermore, the wave to the right of the pond will be called the right wave, analogous to the wave on the left of the pond is called the left wave.

Table 2. The distance of the left and right wave crests to the center of the pond with a non-flat topography

t (s)	Distance to pond center (m)	
	Left wave crest distance	Right wave crest distance
6	2	2
15	1.7	1.7
24	0.58	0.58
33	0.54	0.54
42	1.66	1.66
51	1.18	1.18
60	0.08	0.08

Furthermore, based on the simulation results, data obtained from the crest of the left and right waves to the center of the pond presented in Table 2 and η of the left and right waves have an average difference of 0.0238 m. Based on Table 2, the movement of water flow is not symmetrical, with the distance of the right and left wave crests to the center of the pond having different values in x space units. In addition, the peak velocity of the left and right waves has a difference of 0.0919 m/s. Then, the difference between and the peak velocity of the left and right waves are 0.0238 m and 0.0919 m/s, respectively. Finally, the average value of and wave velocity before reaching the last pond wall until $t = 60$ s is 0.2924 m and 0.1250 m/s, respectively.

3.2. Tsunami Model

The shallow water wave equation can be used to simulate the movement of tsunami waves in the ocean with a long wave initial state. These waves can be caused by the vertical movement of seabed faults, underwater landslides, or the fall of large meteors into the sea. The majority of tsunami waves are caused by the vertical movement of the seabed, which affects the volume of water in the ocean. The description of tsunami waves entirely refers to [1].

The acceleration of gravity g of 9.8 m/s^2 or 127137.6 km/hour^2 was used. The observation area has a length of L (in kilometres (km)), with the computational domain of space variables being [0, L]. The tsunami waves that will be observed are waves that move from $x = 2$ to $x = 10$. The space limit $x = 0$ (on the far left) is the position close to the source of the tsunami wave. Then, the space boundary $x =$ L (on the far right) is the position close to the beach. The simulation was carried out for t (in hours) with the time variable's computational domain being [0, T]. Because the observations are only made on a small part of the ocean area, the boundary conditions used are the free boundary conditions for η and u. The free boundary condition in this experiment caused water on the surface to not move back towards the centre of the tsunami source.

In the tsunami model, two experiments were conducted, namely on tsunami waves on the high seas, which were assumed to have a flat topography, and waves approaching the coast, which have a non-flat topography. To simplify numerical calculations, one unit of space in the simulation was equal to 50 km of actual size. In this model, the length of a unit of space and time was 50 km and 1 hour, respectively.

3.2.1. Flat Topography

It was given a tsunami problem with a flat topography on the one-dimensional (1D) shallow water wave equation. The depth of water under the x-axis follows the functions

$$D(x) = 0.047459, \ 0 \le x \le 10.$$

With the initial conditions for η and u shaped $\eta(x, 0) = 0.001e^{-(x-2)^2}$ and $u(x, 0) = 0.02$ for each $0 \le x \le 10$. Based on the initial conditions, it is known that the initial speed of the waters is 1 km/hour. Furthermore, the spread of tsunami waves was observed for 1 hour using the free boundary conditions. Thus, the

computational domain used in the experiment was [0,10]×[0,1]. The discretization of the initial and boundary conditions can be written as

$$\eta_i^0 = 0.001e^{-(x_i-2)^2}$$
$$u_i^0 = 0.02$$
$$\quad ; i = 0,1,2, \dots , N_x, \tag{10}$$

and

$$\eta_0^n = \eta_1^n, \eta_{N_x}^n = \eta_{N_x-1}^n$$
$$u_0^n = u_1^n, u_{N_x}^n = u_{N_x-1}^n$$
$$\quad ; i = 0,1,2, \dots , N_t, \tag{11}$$

with $N_x = 1000$ and $N_t = 1500$ so that the grid size is obtained $\Delta x = 0.01$ and $\Delta t = \frac{1}{1500}$. The topography of the seabed and the initial state of the water surface are presented in Figure 8. Furthermore, the MacCormack method was used to perform numerical calculations for this experiment. The results of the numerical simulation of the pond model in this experiment when $t = 0;0.15;0.33;0.67;0.95;1$ are presented in Figure 9. The simulation results are only shown at the upper water depth, which is above the y = -0.001 line, without showing the entire area. observation. If it is displayed as a whole, then the wave distribution was difficult to observe. This is because the wave has a very small amplitude compared to the magnitude of D(x).
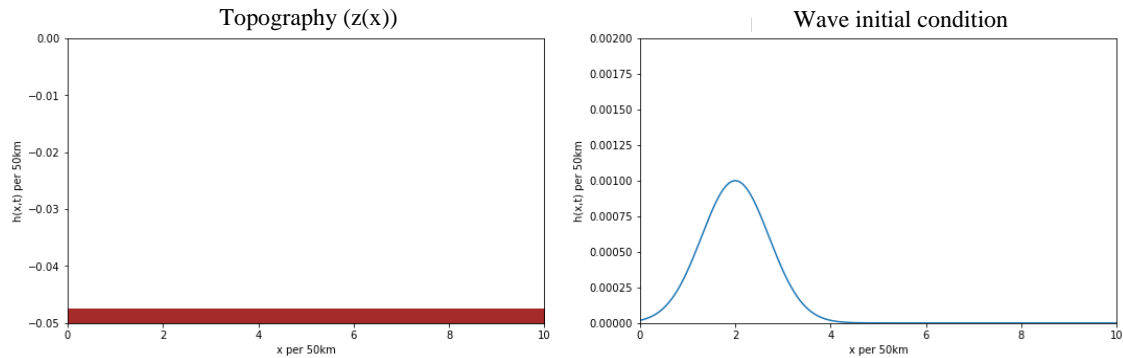

Figure 8. Topography of the seabed (left) and initial state of the water surface (right) for a tsunami model on the high seas

Based on the simulation results, the data obtained are water depth, wave crest height, wave length, and water surface velocity. Based on Figure 9, when the wave moves, the wave has a crest height that does not change, which is 0.02493 km. As a result, the amplitude of the wave also does not change. The free boundary condition in this experiment causes the water on the surface, which reaches the observation limit, will not to move back towards the source of the tsunami. This phenomenon occurs after 0.6 hours, as when $t = 0.67$ hours. When the waves leave the observation area, the water surface becomes calm again as it was at $t = 0.95$ hours with a fixed depth or water level of 2.37342 km. Furthermore, the wavelength data from the simulation results can be presented in tabular form as in Table 3. Based on the table, the wavelength, in this case, has not changed, which is 183 km.
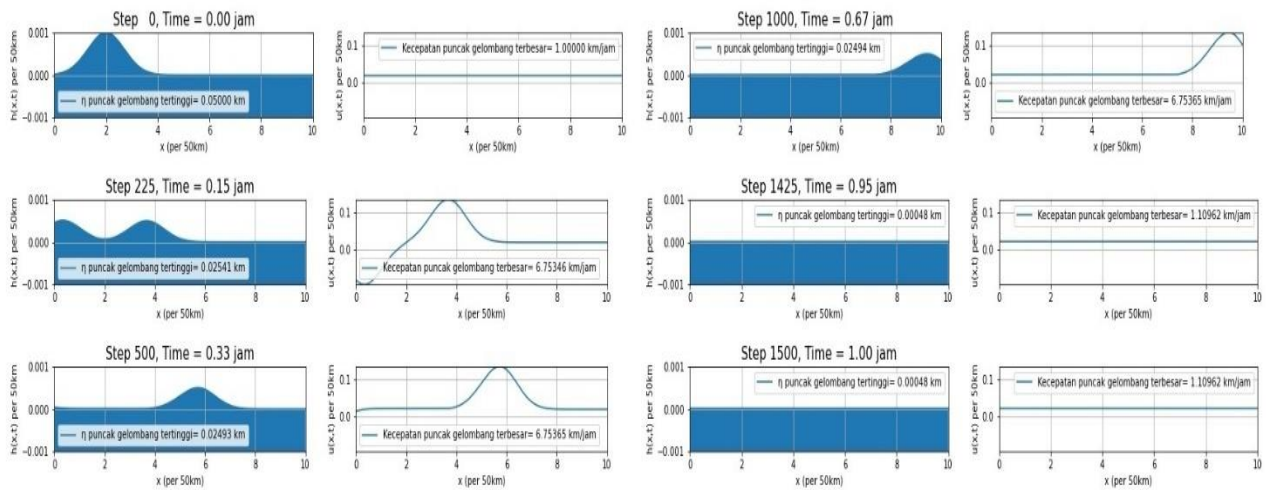
Figure 9. Depth (left) and velocity (right) of water at the water surface in 1 hour for a tsunami model on the high seas

Furthermore, the speed changes that occur in the simulation was observed. At first, the water surface has a 1 km/hour speed. After that, there is a change in speed when the initial wave begins to move. This last for 0.15 hours. Then, the tsunami wave travels to the right with a wave peak speed that tends to remain constant, around 6.754 km/hour. The data is obtained from the simulation results before the wave crest leaves the observation area. After 0.95 hours, all waves have left the observation area, and the water surface has a constant speed of 1.10962 km/hour, which is close to the initial speed of the water surface.

Table 3. Wavelengths for nearshore tsunami models

t (hour)	Wavelength (km)
0.2	183
0.3	183
0.4	183
0.5	183
0.55	183

Based on the simulation results, the data obtained from the speed of the hind legs of the wave or hereinafter referred to as the wave speed and the distance travelled by the wave are presented in Table 4. the average increases by 55.083 km for every 0.1 hour move. After $t = 0.3$ hours, the distance travelled for 0.1 hours has a fixed value of 55 km.

Table 4. Wave velocities for nearshore tsunami models

t (hour)	Wave Speed (km/h)	Wave Distance (km)
0.2	1.20527	19
0.3	1.20512	73.5
0.4	1.20465	128.5
0.5	1.20419	183.5
0.6	1.20372	238.5
0.7	1.20326	293.5
0.8	1.20238	348.5

3.2.2. Non-flat Topography

A tsunami problem with a flat topography was given on the one-dimensional (1D) shallow water wave equation. The depth of water under the x axis follows the function

$$D(x) = 0.047459, \ 0 \le x \le 10.$$

The Initial conditions for η and u is in the form of $\eta(x,0) = 0.001e^{-(x-2)^2}$ and $u(x,0) = 0.02$ for each $0 \le x \le 10$. Based on the initial conditions, it is known that the initial speed of the waters is 1 km/hour. Furthermore, the spread of tsunami waves will be observed for 1 hour using the free boundary conditions. Thus, the computational domain used in the experiment is $[0,10] \times [0,1]$. Discretization of the initial and

boundary conditions, respectively, as in equation (10) and (11) with $N_x = 1000$ and $N_t = 1500$ so that it was obtained size grid $\Delta x = 0.01$ and $\Delta t = \frac{1}{1500}$.
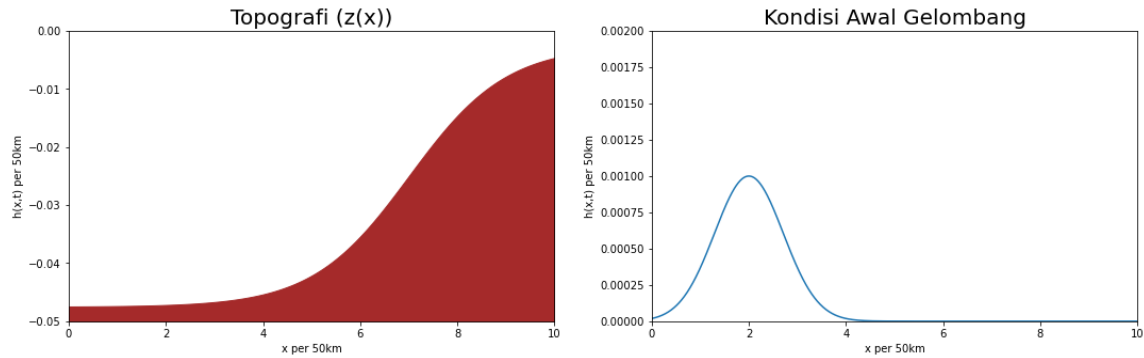

Figure 10. Topography of the seabed (left) and initial state of the water table (right) for a nearshore tsunami model

The topography of the seabed and the initial state of the water surface are presented in Figure 10. Because the observation area is close to the coast, this causes the topography of the seabed to increase as the coast gets closer. Furthermore, the MacCormack method was used to perform numerical calculations for this experiment. The results of the numerical simulation of the pond model in this experiment when $t = 0; 0.15; 0.33; 0.67; 0.95; 1$ are presented in Figure 11. The simulation results are only shown at the upper water depth, which is above the line $y = -0.001$, without showing the entire observation area. If displayed as a whole, then the wave distribution will be difficult to observe. This is because the waves have very small amplitudes compared to amount of $D(x)$.
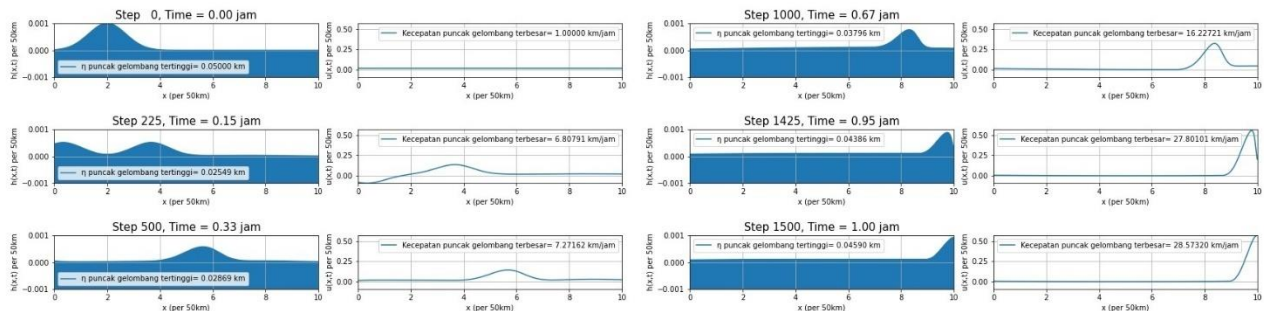

Figure 11. Depth (left) and velocity (right) of water in waters in 1 hour for the nearshore tsunami model

Based on the simulation results, the obtained data are water depth, wave crest height, wave length, and water surface velocity. After 0.15 hours, the long wave moves in two directions, approaching and away from the beach. In particular, only waves approaching the coast will be discussed. In the topography of the seabed in Figure 10, the topography has not experienced a large increase at $0 \leq x \leq 4$, in contrast to the topography at $4 \leq x \leq 10$. The average height of the tsunami wave crest, calculated from the x-axis, at $2 \leq x \leq 4$ is about 0.02561 km or 25.61 m. Although the change in height is very small, the wave crest increases. At $t = 0.33$ hours, the wave's crest has a height of 0.02869 km. Then, at $t = 1$ hour, the wave's crest has a height of 0.04186 km. As a result, it is known that the wave amplitude gets bigger as the topography increases. The free boundary condition of the tsunami model means that water on the surface will not move back toward the source of the tsunami. This phenomenon occurs after 0.9 hours, as at $t = 0.95$ hours. Wavelength data from the simulation can be presented in tabular form as in Table 5. Furthermore, based on Table 5, it is found that the wavelength has decreased and is directly proportional to the distance of the tsunami waves to the coast.

Table 5. Wavelengths for nearshore tsunami models

t (h)	Wavelength (km)
0.2	163.5
0.35	145
0.5	126.5
0.65	100
0.8	84

Based on Figure 10, the velocity of the water surface is always changing. At $t = 0.15$, the wave's crest has a speed of about 6.80791 km/hour. Then at $t = 1$, the wave crest has a speed of about 28.57320 km/hour. The peak speed of the wave has increased. Then, based on the simulation results, the data obtained for the speed and distance of the waves are presented in Table 6. Based on Table 6, the wave speed decreased, and the average wave distance increased by 44.16 km for every 0.1 hour movement. As previously described, a decrease in wave speed causes the wavelength to decrease and the amplitude to increase. After $t = 0.3$ hours, the distance moved for 0.1 hours has a different value and decreases.

Table 6. Wave velocities for nearshore tsunami models

t (h)	Wave Speed (km/h)	Wave Distance (km)
0.2	1.0360	10
0.3	0.8774	63
0.4	0.5684	117
0.5	0.2934	168.5
0.6	0.1032	216
0.7	0.0260	257.5
0.8	0.0248	275

4. CONCLUSION

In this article, numerical simulations using the MacCormack method have been carried out for 1D shallow water wave pond and tsunami models. The pond and tsunami models are discussed for the cases of flat and non-flat topography, respectively. Based on the results of numerical simulations that have been carried out, several conclusions were obtained as follows:

1. In the pond model, the water surface for flat topography moves symmetrically to the center of the pond, while for non-flat topography it moves asymmetrically.

2. In the pond model for flat topography, wave amplitude and velocity are greater than the wave amplitude and velocity for non-flat topography.

3. In the tsunami model, the tsunami waves in the case of a flat topography propagate faster than the tsunami waves in the case of a non-flat topography.

4. In the tsunami model, the tsunami wave has a fixed shape in flat topography, while the tsunami waves changes shape in the case of non-flat topography. The shape changes include the amount of amplitude and the length of the wave.

As a result, it can be concluded that the topographical shape can affect the movement of the water surface.

REFERENCES

[1] A. Trujillo and H. Thurman, Essentials of Oceanography, Boston: Pearson, 2016.

[2] M. Jamhuri, "Simulasi Perambatan Tsunami menggunakan Persamaan Gelombang Air Dangkal [Simulation of Tsunami Propagation using the Shallow Water Wave Equation]," Universitas Islam Negeri Maliki, Malang, 2014.

[3] S. Hati, K. Yulianti and R. Marwati, "Simulasi Sistem Persamaan Gelombang Air Dangkal Menggunakan Metode Numeris Lax-Friedrichs [Simulation of Shallow Water Wave Equation System Using Lax-Friedrichs . Numerical Method]," *Jurnal Eureka Matika,* vol. 8, 2020.

[4] D. Prayitno and Sumardi, "Simulations of shallow water equations by finite difference WENO schemes with multilevel time discretization," *AIP Conference Proceedings,* vol. 2268, no. 1, 2020.

[5] S. R. Pudjaprasetya and I. Magdalena, " Momentum Conservative Schemes for Shallow Water Flows," *East Asian Journal on Applied Mathematics,* 2013.

[6] H. P. Gunawan, "Numerical Simulation of Shallow Water Equations and Related Models," HAL, 2015.

[7] R. Setiyowati and Sumardi, "A Simulation of Shallow Water Wave Equation Using Finite Volume Method: Lax-Friedrichs Scheme," *Journal of Physics: Conference Series,* vol. 1306, 2019.

[8] P. Crowhurst, "Numerical Solution of One Dimentional Shallow Water Equation," *Australian Mathematical Sciences Institute,* 2013.

[9]   I. Wahidah, " Simulasi Numerik Model Sisko Untuk Aliran Darah Tak-Tunak Dalam Pembuluh [Numerical Simulation Sisko Model for Unsteady Blood Flow in Vessels]," Universitas Gadjah Mada, Yogyakarta, 2018.

[10] N. Pochai, "Numerical treatment of a modified MacCormack scheme in a nondimensional form of the water quality models in a nonuniform flow stream," *Journal of Applied Mathematics,* 2014.

[11] N. L. H. Zendrato, A. Chrysanti, B. P. Yakti, M. B. Adityawan, Widyaningtias and Y. Suryadi, "Application of Finite Difference Schemes to 1D St. Venant for Simulating Weir Overflow," in *MATEC Web of Conferences*, 2018.

[12] E. Ngondiep, A. Rubayyi and J. C. Ntonga, "A MacCormack Method for Complete Shallow Water Equations with Source Terms," *American Mathematical Society,* no. 65, 2019.

[13] M. A. Abdelrahman, "On the Shallow Water Equations," *Zeitschrift fur Naturforschung a,* vol. 72, no. 9, pp. 873-879, 2017.

[14] H. S. Shaw, "Numerical Modelling of Tsunami Wave Equations," National Institute of Technology Rourkela, 2014.

[15] P. R. Pinet, Invitation to Oceanography Seventh Edition, Jones & Bartlett Publisher, 2014.